Revised phase diagram for the FeTe_{1-x}Se_{x} system with fewer excess Fe atoms

Chiheng Dong, Hangdong Wang, Zujuan Li, Jian Chen, H. Q. Yuan, and Minghu Fang

Phys. Rev. B **84**, 224506 — Published 15 December 2011

DOI: 10.1103/PhysRevB.84.224506

Revised Phase Diagram for $FeTe_{1-x}Se_x$ system with less excess Fe atoms

Chiheng Dong,[1] Hangdong Wang,[1,2] Zujuan Li,[1] Jian Chen,[1] H. Q. Yuan,[1] and Minghu Fang[1,*]

[1] *Department of Physics, Zhejiang University, Hangzhou 310027, China*
[2] *Department of Physics, Hangzhou Normal University, Hangzhou 310036, China*

(Dated: November 14, 2011)

We observed bulk superconductivity in the $FeTe_{1-x}Se_x$ crystals with lower Se concentrations after annealed in air. A revised magnetism and superconductivity phase diagram is obtained via resistance and magnetic susceptibility measurements for the $FeTe_{1-x}Se_x$ system. It is found that bulk superconductivity coexists with antiferromagnetic order in the crystals with $0.05 \leq x \leq 0.18$. The phase diagram is very similar to the case of the K-doping or Co-doping $BaFe_2As_2$, as well as of the $SmFeAsO_{1-x}F_x$ system, perhaps indicating that all the iron-based systems have a generic phase diagram, although the antiferromagnetic wave vectors in the parent compounds of both iron pnictides and $FeTe_{1-x}Se_x$ systems are remarkably different.

PACS numbers: 74.70.Xa,74.25.Dw,74.62.Bf

I. INTRODUCTION

The discovery of superconductivity (SC) in the iron pnictides has generated great interest in understanding the interplay of magnetism and SC in the iron-based layered compounds[1,2]. There are, so far, four different structural classes of Fe-based compounds reported, *i.e.*, 1111-type ReOFeAs (Re=rare earth)[3–7], 122-type AFe_2As_2 (A=Ba, Sr, or Ca)[8,9], 111-type BFeAs (B=alkali metal)[10–12] and 11-type Fe(Te, Se, S)[13–16]. Their magnetic and superconducting phase diagrams are qualitatively similar to those of several other classes of unconventional superconductors, including the cuprates[17,18], organics[19,20] and heavy-fermion superconductors[21,22]. In all these cases, the antiferromagnetic (AFM) order must be suppressed, either by doping or pressure, before optimal bulk SC appears. But, up to now, it has also been found that there are somewhat differences in the details of the phase diagram among the Fe-based systems. For the fluorine-doped '1111' systems such as $LaFeAsO_{1-x}F_x$[23], the AFM and SC phases are completely separated and do not overlap. In the $BaFe_2As_2$, the systematic substitution of either the alkaline-earth (Ba)[24,25], transition-metal (Fe)[26,27] or pnictogen (As)[28] atom with different elements almost universally produces the phase diagram which is composed of coupled AFM and structural transitions that are suppressed with substitution and an SC phase that is more or less centered near the critical concentration where AFM order is destroyed. The phase diagram obtained from the $Fe_{1+y}Te_{1-x}Se_x$ system[29–31], up to now, is somewhat different from that of the 1111 and 122-type systems, containing a spin glass region between the AFM and SC phases. Long-range AFM order ceases at $x = 0.1$, and bulk SC does not set in until x exceeds 0.3.

There is another important characteristic in the $Fe_{1+y}Te_{1-x}Se_x$ system which is different from the Fe-pnictide (1111- and 122-type) system. The parent compounds of the Fe-pnictide are in a collinear AFM order, characterized by an in-plane propagation wave-vector $Q_n = (\pi,\pi)$[23,32,33]. $Fe_{1+y}Te$, the parent compound of the $Fe_{1+y}Te_{1-x}Se_x$ superconductors, is in a bi-collinear AFM order, characterized by an in-plane propagation wave-vector $Q_m = (\pi,0)$[34,35], although both the doped iron-pnictide[36–39] and iron-chacolgenide[40] superconductors exhibit a magnetic response around the same wave vector (π,π) in the spin excitation spectra in the superconducting state. Thus, it was suggested[29–31] that there is an intermediate region with magnetic correlations near $(\pi,0)$, which are not favorable to SC, in the phase diagram, between the long-range $(\pi,0)$ magnetic order phase and the SC phase with (π,π) magnetic resonance. However, the presence of excess Fe atoms in the $Fe_{1+y}Te_{1-x}Se_x$ system results in an incommensurate AFM order[34] and may provide a magnetic pair breaking effect[41]. In this article, we annealed the $FeTe_{1-x}Se_x$ crystals in air, which may partially remove the excess Fe atoms existing unavoidably in the crystals as-grown, especially for that with a less Se concentrations, and found that there is no intermediate region in the phase diagram for the $FeTe_{1-x}Se_x$ system with less excess Fe atoms. Instead, the SC phase with (π,π) magnetic resonance can coexist with the long-range $(\pi,0)$ magnetic order phase in a rather wide Se concentration range. The surprisingly similarity of the phase diagram of the $FeTe_{1-x}Se_x$ system with less excess Fe atoms to that of the doping $BaFe_2As_2$ system, as well as the $SmFeAsO_{1-x}F_x$ system reported recently[42], indicates that the coexistence of AFM and SC phases is probably a more intrinsic property of the generic phase diagram in the Fe-based superconductors .

II. EXPERIMENTAL DETAILS

Single crystals of $Fe_{1+y}Te_{1-x}Se_x$ were grown using the Bridgman method. A mixture of Fe(99.99%), Te(99.999%), and Se(99.999%) powders with appropriate ratios was loaded into a silica Bridgman ampoule and sealed into a second one to avoid the crack upon cooling. The ampoule was evacuated, sealed and heated to 920 ℃, then slowly cooled to room temperature. The single crystals as-grown with typical size of 5.0×5.0×1.0 mm^3 (as shown in the inset of Fig. 1 (d)) can be easily cleaved perpendicular to the c axis. We cleaved them into thin slices (2.0×1.0×0.2 mm^3) and re-heat them under three types of circumstances to compare the annealing effects on their properties: firstly, only in air at different temperatures ($\leq$ 300℃) for 2 hours (noted by A); secondly, only in vacuum at 400 ℃ for 7 days (V); thirdly, both in vacuum and in air (V+A). We found that the color of the crystals annealed in air changes to blue (see the right inset of Fig. 1 (d)), instead, there is no change in the color of the crystals annealed in vacuum, which have the same reflective shinning surface as the crystals as-grown (left inset of Fig. 1 (d)).

The average composition was determined on at least 10 regions of the crystal by the Energy-dispersive X-ray (EDXS) method with the Phoenix EDAX equipment attached to a field-emission scanning electron microscope (SIRION FEI). We always chose a fresh surface, cleaved from the crystals as-grown, annealed, as well as the multiple cleaved crystals annealed in air to determine the intrinsic Fe content. Within the precision of our EDXS experiments, no remarkable difference of the Fe content was observed on different inner surfaces of the same crystal, nor on the different crystals annealed in air in the same batch. We found that the Fe content in the crystals annealed in air is indeed a little less than that in the crystals as-grown and annealed only in vacuum, as shown in Table 1. Instead, the Fe content of the crystals annealed only in vacuum is almost the same as that of the crystals as-grown. We suspect that the excess Fe atoms partially occupying the interstitial Fe(2) sites, which was confirmed by the neutron diffraction experiments[34],

TABLE I. Chemical compositions, lattice parameters before and after annealing of the $FeTe_{0.9}Se_{0.1}$ and $FeTe_{0.6}Se_{0.4}$ single crystals. The chemical compositions were derived from EDXS. The lattice constants were determined by fitting the powder X-ray diffraction patterns.

Nominal composition	annealing condition	average composition (±0.02)	a (Å)	c (Å)
$FeTe_{0.9}Se_{0.1}$	as-grown	$Fe_{1.10}Te_{0.91}Se_{0.09}$	3.820(3)	6.247(3)
	400 ℃ V	$Fe_{1.10}Te_{0.90}Se_{0.10}$	3.819(1)	6.247(1)
	270 ℃ A	$Fe_{1.06}Te_{0.90}Se_{0.10}$	3.826(3)	6.245(3)
$FeTe_{0.6}Se_{0.4}$	as-grown	$Fe_{1.01}Te_{0.56}Se_{0.44}$	3.806(3)	6.068(3)
	400 ℃ V	$Fe_{1.01}Te_{0.55}Se_{0.45}$	3.805(1)	6.076(1)
	270 ℃ A	$Fe_{1.00}Te_{0.56}Se_{0.44}$	3.804(3)	6.069(3)

and combining weakly with the Se atoms, are easily removed out and oxidized as the crystals are annealed in air.

The single crystal and powder X-ray diffractions were performed at room temperature using a D/Max-rA diffractometer with Cu-K_α radiation and a graphite monochromator. The resistance was measured using the standard four probes method with a Quantum Design Physical Property Measurement System (PPMS-9). The magnetization was measured on a Quantum Design Magnetic Property Measurement System (MPMS-5).

III. RESULTS AND DISCUSSIONS

At first, we discuss the effects of annealing under different circumstances on the properties of the single crystals with a lower ($x = 0.1$) and a higher ($x = 0.4$) Se concentration. According to the EDXS results (shown in Table 1), the excess Fe in the $Fe_{1+y}Te_{0.9}Se_{0.1}$ crystals as-grown is more than that in the $Fe_{1+y}Te_{0.56}Se_{0.44}$ crystals as-grown, which is consistent with that the excess Fe decreases with increasing Se concentration[43,44]. Single crystal X-ray diffraction (XRD) pattern for the crystal as-grown with x=0.1 (Fig. 1 (d)), only shows the ($00l$) peaks, indicating that the crystallographic c axis is perpendicular to the plane of the crystals. The XRD patterns for the powders by grinding many pieces of crystals annealed at 270 ℃ for 2 hours in air, annealed at 400 ℃ for 7 days in vacuum and as-grown are shown in Fig. 1 (a) (b) and (c), respectively. There is no remarkable difference in the positions of the diffraction peaks for these crystals, and there are some impurity peaks of Fe_7Se_8 in the XRD patterns, which may exist between the crystals. The lattice parameters were obtained by fitting the powder XRD data (Table 1). It's difficult in our XRD experiments to detect the changes of lattice parameters due to the small amount of removed excess Fe atoms.

Figure 2 presents the temperature dependence of the normalized in-plane resistance, $R(T)$, and DC susceptibility, $\chi(T)$, measured at 5 Oe ($\|ab$ plane for reducing the demagnetization effect) with zero-field-cooling (ZFC) procedure for the crystals with x=0.1, 0.4 before and after annealed. For the $Fe_{1+y}Te_{0.9}Se_{0.1}$ crystals as-grown and annealed only in vacuum, as shown in the insets in Fig. 2(a), their resistivity and susceptibility data do not show any superconducting transition above 2 K. But all the $FeTe_{0.9}Se_{0.1}$ crystals annealed in air at different temperatures, and the crystals annealed both in air and vacuum exhibit bulk SC below 8 K. According to the susceptibility measurement, the superconducting volume fraction (SVF) increases with increasing annealing temperature [see the right inset of Fig. 2(a)], *i.e.*, SVF is of 7 % for the crystals annealed at 200 ℃, 30 % for 270 ℃, 50 % for both in vacuum at 400 ℃ for 7 days and in air at 270 ℃ for 2 hours, indicating bulk SC, instead of surface effect. There is a kink at about T_N=38 K, corresponding to an AFM transition, in the $R(T)$ curves for all the crystals. We found that annealing in air and vacuum has little effect on $R(T)$ behavior above T_N, but results in a slight decrease of T_N (38 K for the crystals annealed in air at 270 ℃, while 42 K for the crystals as-grown). The $R(T)$ above T_N exhibits a semiconducting behavior for all the crystals. The result of the coexistence of bulk SC and an AFM order in $FeTe_{0.9}Se_{0.1}$ crystals annealed in air is sharply inconsistent with that reported in Refs. 30 and 31. On the basis of our EDXS data, we found that Fe content decreases from 1.10 in the crystals as-grown to almost 1.06 in the crystals annealed in air at 270 ℃, but there is little change in the relative ratio of Te and Se before and after annealed. In contrast, the annealing in vacuum does not result in the decrease of Fe content.

Although the reduction of the content of excess Fe atoms is not so obvious for $Fe_{1+y}Te_{0.6}Se_{0.4}$ (Table 1), we found that annealing also improve its SC. Figure 2(b) presents the temperature dependence of the in-plane normalized resistance, $R(T)$, and DC susceptibility, $\chi(T)$, for the $FeTe_{0.6}Se_{0.4}$ crystals as-grown, and annealed. For the crystals as-grown, although its $R(T)$ data shows a superconducting transition with ${T_c}^{onset}$ = 13 K, ${T_c}^{zero}$ = 10 K, the SVF is very small (∼5%), as shown in the right inset of Fig. 2(b), and its $R(T)$ at the normal state exhibits a semiconductor-like behavior. For the crystal annealed only in vacuum, both the $R(T)$ and $\chi(T)$ data show that the crystal exhibits bulk SC with ${T_c}^{onset}$=13.7 K, ${T_c}^{zero}$=11.3 K, the T_c and SVF (76 %) are higher than those in the

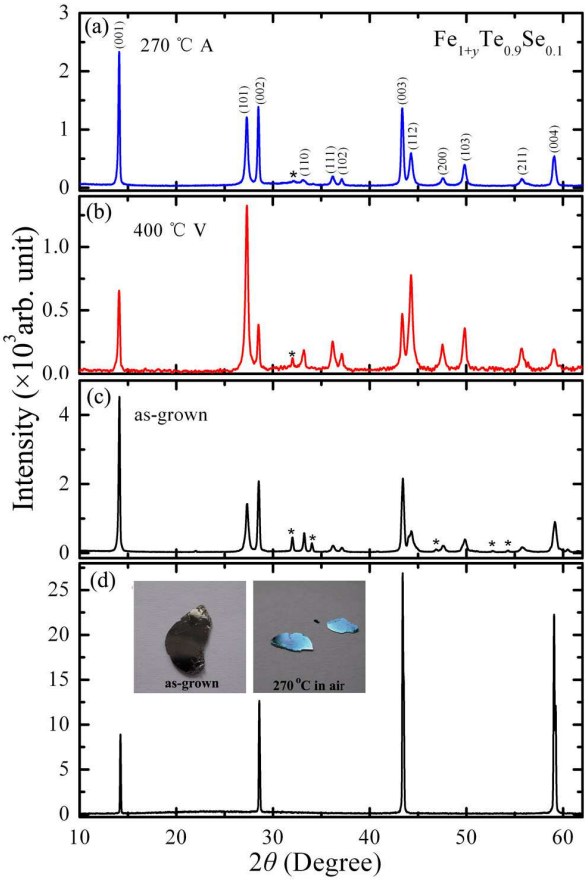

FIG. 1. (Color online) X-ray diffraction (XRD) patterns of the $FeTe_{0.9}Se_{0.1}$ powders obtained by grinding many pieces of crystals (a) annealed at 270 ℃ for 2 hours in air, (b) annealed at 400℃ for 7 days in vacuum, (c) as-grown, the asterisks indicate the impurity phase of Fe_7Se_8, (d) Single crystal XRD for the $FeTe_{0.9}Se_{0.1}$ crystal as-grown. The inset are the photos for the crystal as-grown (Left) and the crystals (Right) annealed at 270℃ in air.

crystals as-grown, and its $R(T)$ at the normal state shows a metallic behavior. For the crystals with a higher Se concentration, annealing in vacuum can improve not only SC but also transport properties at the normal state. T. Taen et al.[45] have confirmed that the inhomogeneity of Se/Te is greatly depressed by annealing in vacuum for the $FeTe_{0.61}Se_{0.39}$ crystal. This result indicates that the inhomogeneity of Se/Te distribution in the crystals, especially for the crystals with higher Se concentrations, is another factor to suppress SC except for the magnetic pair-breaking effect resulting from the interstitial Fe atoms in the $Fe_{1+y}Te_{1-x}Se_x$ system.

Also, for all the $FeTe_{0.6}Se_{0.4}$ crystals annealed only in air, although their $R(T)$ at the normal state still shows a similar semiconductor-like behavior as that in the crystal as-grown, their SC is remarkably improved, and the T_c and SVF increase with increasing annealing temperature, *i.e.*, SVF is of 5 % for the crystals as-grown, 28 % for the crystals annealed at 200 ℃, 40 % for 270 ℃, 70 % for 300 ℃, close to the SVF value of 76 % for the crystals annealed only in vacuum, the SVF increases to 94 % for the crystals annealed both in vacuum at 400 ℃ for 7 days and in air at 270 ℃ for 2 hours. These results indicate that the existence of excess Fe atoms is the main factor to suppress SC, even in the crystals with higher Se concentrations. The inhomogeneity in the crystals not only results in the semiconductor-like behavior at the normal state but also suppress SC for the samples with higher Se concentrations, but it is not the main factor in the crystals with lower Se concentrations. The $R(T)$ and $\chi(T)$ data for the crystals annealed first in vacuum, then in air present an evidence for this scenario, which has the highest ${T_c}^{mid}$=15.2 K with the sharpest transition, the largest SVF ($\sim$ 100%), and its $R(T)$ at the normal state exhibits also a metallic behavior.

On the basis of the results above, we can conclude that annealing only in air is always effective in the crystals with higher and lower Se concentrations. Our EDXS data show that the Fe content in the crystals annealed in air, especially for the crystals with a lower Se concentration, is less than that in the crystals as-grown or annealed only in vacuum, indicating that the excess Fe atoms is partially removed by annealing in air. Of course, the annealing in air or in vacuum may result in the suppression of the inhomogeneity of Se/Te distribution and release of the stress in the

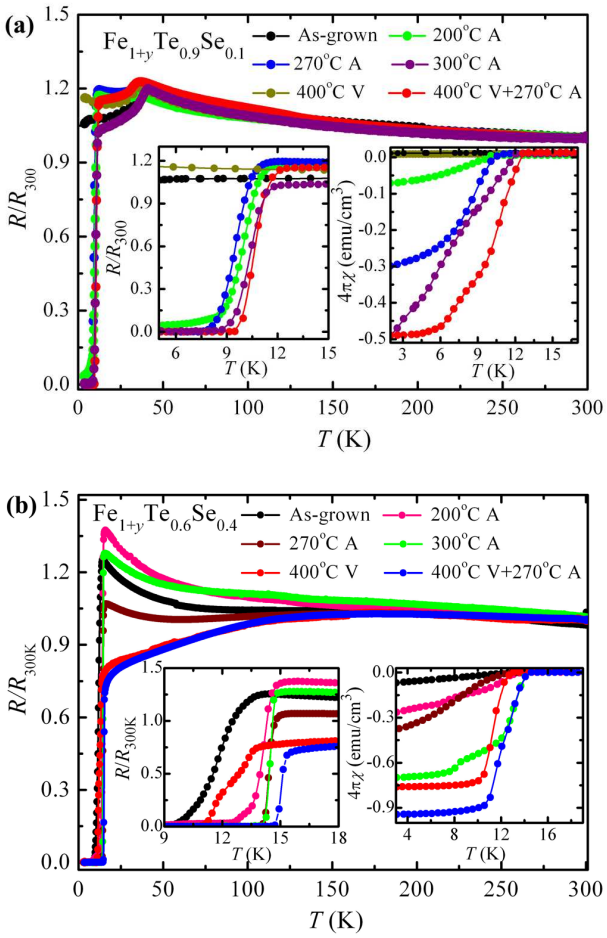

FIG. 2. (Color online) (a) Temperature dependence of the in-plane normalized resistance, R/R_{300K} (main plot), the left inset shows their data near T_c, the right inset plots the susceptibility as a function of temperature, $\chi(T)$, measured at 5 Oe ($\|ab$) with ZFC for the $FeTe_{0.9}Se_{0.1}$ crystals as-grown and annealed at different temperatures in air (A) and in vacuum (V). (b) R/R_{300K}, (main plot), the left inset shows their data near T_c, the right inset plots $\chi(T)$ for the $FeTe_{0.6}Se_{0.4}$ crystals as-grown and annealed at different temperatures in air and in vacuum.

crystals. As discussed above, annealing only in vacuum improves SC in the crystals with a higher Se concentration, but it's not effective for that with low Se concentrations. So, we suggest that the excess Fe atoms are the main factor to suppress SC in this system, while the inhomogeneity or stress may be other factors to suppress SC in the crystals with higher Se concentrations.

Figure 3(a) and 3(b) show the normalized in-plane resistance and the DC susceptibility of the crystals with different Se concentrations. All of these single crystals were annealed at 270 ℃ for 2 hours. For the crystals with $x = 0$, and 0.02, a sharp decrease in resistance are observed at $T_N = 70$, 62.6 K, respectively, corresponding to the AFM transition, companied with a structural transition, as reported in our original papers[14,34], but there is no drop corresponding to a SC transition observed above 2 K. For the crystals with $x = 0.05$, 0.07, and 0.1, except for a sharp decrease in resistance at T_N, which decreases with increasing Se concentration, another sharp drop corresponding to a SC transition is observed at T_c(mid) = 6.7, 8.2, and 9.6 K, respectively, zero resistance is obtained at $T_c{}^{zero} = 4.0$ and 7.6 K for the $x = 0.07$, 0.1 crystals, but no zero resistance obtained for $x = 0.05$ above 2 K. To check whether SC in the crystals with lower Se concentration annealed in air is a bulk property or not, we measured their bulk susceptibility, as shown in the right inset in Fig. 3(b). For the crystals with $0.07 \leq x \leq 0.4$, both the resistance and susceptibility data show that bulk SC exists in these crystals. As discussed above, the SVF is at least up to 30 % for the $x = 0.1$ crystal annealed in air at 270 ℃, although their SC transition in the $\chi(T)$ is not so sharp, and the SVF is smaller than that in the crystal with x= 0.4 annealed both in vacuum and in air. It is remarkable that the temperature dependence of resistance exhibits a semiconductor-like behavior above the SC transition. Although there is no drop in resistance corresponding to an AFM transition at T_N for the crystals with $0.12 \leq x \leq 0.18$, a drop in the bulk susceptibility measured at 1 Tesla with field cooling (FC) procedure confirms this transition, as shown in the right

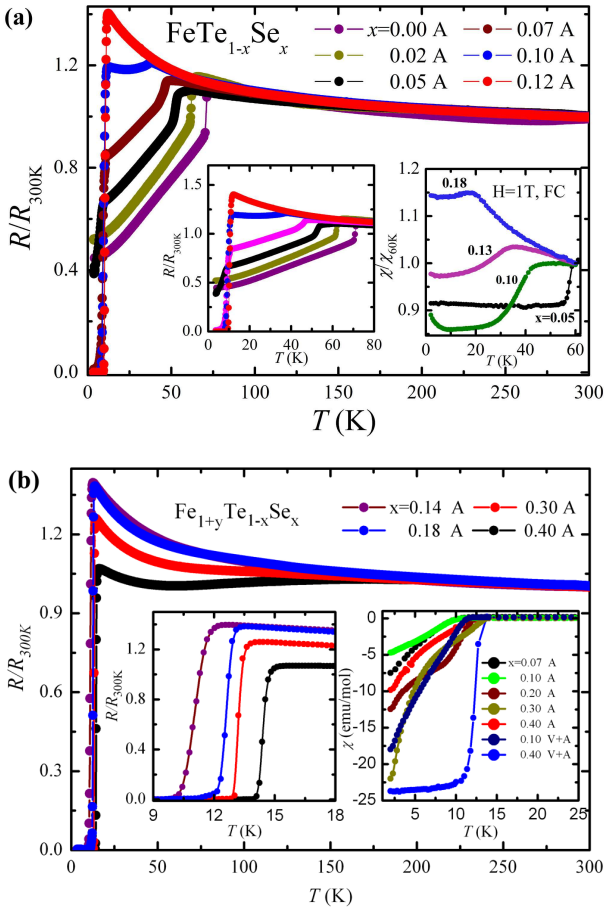

FIG. 3. (Color online)Temperature dependence of the in-plane normalized resistance, R/R_{300K}, for the $FeTe_{1-x}Se_x$ crystals annealed at 270 ℃ in air (A). (a) $0 \leq x \leq 0.12$, the left inset shows their data at lower temperatures. (b) $0.14 \leq x \leq 0.4$, the left inset shows their data at lower temperatures. The right inset in (a): temperature dependence of the normalized susceptibility, χ/χ_{60K}, measured at 1 *Tesla* ($\|c$) with FC procedure, for the $x = 0.05$, 0.10, 0.13 and 0.18. The right inset in (b): temperature dependence of the susceptibility, χ(T), measured at 5 Oe ($\|c$) with ZFC procedure for the $x = 0.07$, 0.10, 0.20, 0.30, and 0.40 crystals.

inset of Fig. 3(a).

The result of the coexistence of bulk SC and long-range AFM order in the $FeTe_{1-x}Se_x$ crystals with a low Se concentration, is sharply inconsistent with that reported previously[29–31]. We suspect that the difference in the amount of the excess Fe atoms existing unavoidably in the crystals with a lower Se concentration may result in these disagreements. We also found that the crystals as-grown and annealed only in vacuum with $x \leq 0.3$ indeed do not show bulk SC.

Figure 4 shows the x-T phase diagram based on the resistance and susceptibility data for the $FeTe_{1-x}Se_x$ crystals annealed in air at 270 ℃ for 2 hours. The value of x is a nominal value and may not be exactly correct. The EDXS data show that the Se concentration x is almost the same as the nominal value, and the Fe concentration in the crystals annealed in air is closer to unity than that in the crystals as-grown or annealed in vacuum. The T_N is determined by the temperature at which both $\mathrm{d}R(T)/\mathrm{d}T$ and $\mathrm{d}\chi(T)/\mathrm{d}T$ have a maximum value. The T_c is determined by the middle temperature of the SC transition in $R(T)$ curves. The phase diagram clearly shows that there is a region ($0.05 \leq x \leq 0.18$) where the AFM phase coexists with bulk SC phase. Of course, we can not conclude that the coexistence between bulk SC and long-range AFM order in the crystals with lower Se concentration is in a microscopic scale, which may also be due to some kind of phase separation. But it is affirmable that the SC observed in these crystals is not a surface effect, because the SVF in the crystals with less excess Fe atoms is up to 50%, as discussed above for the x=0.1 crystal. Our phase diagram of $FeTe_{1-x}Se_x$ is similar to the neutron powder diffraction results of polycrystalline $FeTe_{1-x}Se_x$[44], but much different from the results reported in Refs. 29–31. It is surprising that the bulk SC exhibiting a magnetic response around the wave vector (π,π) coexists with the AFM order characterized by an in-plane wave vector Q_m=(π, 0). Our finding of the similarity of the phase diagram of the $FeTe_{1-x}Se_x$ system to that of the K-

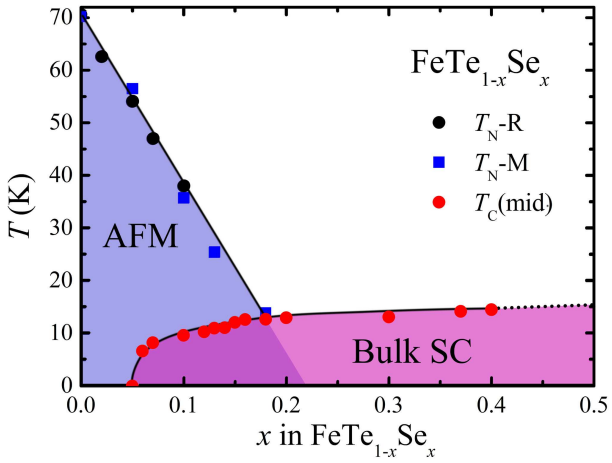

FIG. 4. (Color online)Phase diagram for $FeTe_{1-x}Se_x$ system. The AFM transition temperature, T_N and the superconducting transition temperature T_c as a function of x.

or Co-doping 122-type system, as well as that of the $SmFeAsO_{1-x}F_x$ system reported recently[42], indicates that the coexistence of AFM and SC phases may be an intrinsic property of the Fe-based superconductors.

IV. SUMMARY

In summary, we observed bulk superconductivity in the $FeTe_{1-x}Se_x$ crystals with lower Se concentrations after annealed in air. A revised magnetism and SC phase diagram of $FeTe_{1-x}Se_x$ system with less excess Fe atoms is obtained via resistivity and magnetic susceptibility measurements. It was found that bulk SC coexists with AFM order in the crystals with $0.05 \leq x \leq 0.18$, while it needs further investigation to figure out whether this coexistence is in a microscopic scale or due to some kind of phase separation. The phase diagram is very similar to the case of the K-doping or Co-doping 122 iron-pnictide system, indicating that all iron-based systems have a similar phase diagram, although the AFM wave vectors in the parent compounds of both systems are remarkablely different.

ACKNOWLEDGMENTS

This work is supported by the National Science Foundation of China (Grant No.10974175, 10934005), the National Basic Research Program of China (Grant No.2011CBA00103, 2012CB821404 and 2009CB929104), the PCSIRT of the Ministry of Education of China (Contract No.IRT0754).

* mhfang@zju.edu.cn

[1] Y. Kamihara, T. Watanabe, M. Hirano, and H. Hosono, J. Am. Chem. Soc **130**, 3296 (2008).
[2] X. H. Chen, T. Wu, G. Wu, R. H. Liu, H. Chen, and D. F. Fang, Nature **453**, 761 (2008).
[3] G. F. Chen, Z. Li, D. Wu, G. Li, W. Z. Hu, J. Dong, P. Zheng, J. L. Luo, and N. L. Wang, Phys. Rev. Lett. **100**, 247002 (2008).
[4] Z. A. Ren, W. Lu, J. Yang, W. Yi, X. L. Shen, Z. C. Li, G. C. Che, X. L. Dong, L. L. Sun, F. Zhou, and Z. X. Zhao, Chin. Phys. Lett. **25**, 2215 (2008).
[5] Z. A. Ren, J. Yang, W. Lu, W. Yi, X. L. Shen, Z. C. Li, G. C. Che, X. L. Dong, L. L. Sun, F. Zhou, and Z. X. Zhao, Europhys. Lett. **82**, 57002 (2008).
[6] P. Cheng, L. Fang, H. Yang, X. Y. Zhu, G. Mu, H. Q. Luo, Z. S. Wang, and H. H. Wen, Sci China Ser G-Phys Mech Astron **51**, 719 (2008).
[7] C. Wang, L. Li, S. Chi, Z. Zhu, Z. Ren, Y. Li, Y. Wang, X. Lin, Y. Luo, S. Jiang, X. F. Xu, G. Cao, and Z. Xu, Europhys. Lett. **83**, 67006 (2008).
[8] M. Rotter, M. Tegel, and D. Johrendt, Phys. Rev. Lett. **101**, 107006 (2008).
[9] A. S. Sefat, R. Jin, M. A. McGuire, B. C. Sales, D. J. Singh, and D. Mandrus, Phys. Rev. Lett. **101**, 117004 (2008).
[10] X. C. Wang, Q. Q. Liu, Y. X. Lv, W. B. Gao, L. X. Yang, R. C. Yu, F. Y. Li, and C. Q. Jin, Solid State Commun. **148**, 538 (2008).
[11] J. H. Tapp, Z. Tang, B. Lv, K. Sasmal, B. Lorenz, P. C. W. Chu, and A. M. Guloy, Phys. Rev. B **78**, 60505 (2008).
[12] M. J. Pitcher, D. R. Parker, P. Adamson, S. J. C. Herkelrath, A. T. Boothroyd, R. M. Ibberson, M. Brunelli, and S. J. Clarke, Chem. Commun. **45**, 5918 (2008).
[13] F. C. Hsu, J. Y. Luo, K. W. Yeh, T. K. Chen, T. W. Huang, P. M. Wu, Y. C. Lee, Y. L. Huang, Y. Y. Chu, D. C. Yan, and M. K. Wu, Proc. Natl. Acad. Sci. U.S.A. **105**, 14262 (2008).
[14] M. H. Fang, H. M. Pham, B. Qian, T. J. Liu, E. K. Vehstedt, Y. Liu, L. Spinu, and Z. Q. Mao, Phys. Rev. B **78**, 224503 (2008).
[15] Y. Mizuguchi, F. Tomioka, S. Tsuda, T. Yamaguchi, and Y. Takano, Appl. Phys. Lett. **94**, 012503 (2009).
[16] C. H. Dong, H. D. Wang, J. H. Yang, B. Qian, J. Chen, Z. J. Li, H. Q. Yuan, and M. H. Fang, Sci China Ser G-Phys Mech Astron **53**, 1216 (2010).
[17] A. Damascelli, Z. Hussain, and Z. X. Shen, Rev. Mod. Phys **75**, 473 (2003).
[18] N. P. Armitage, P. Fournier, and R. L. Greene, Rev. Mod. Phys. **82**, 2421 (2010).
[19] S. Lefebvre, P. Wzietek, S. Brown, C. Bourbonnais, D. Jérome, C. Mézière, M. Fourmigué, and P. Batail, Phys. Rev. Lett. **85**, 5420 (2000).
[20] B. J. Powell and R. H. McKenzie, Phys. Rev. Lett. **94**, 047004 (2005).
[21] T. Park, F. Ronning, H. Q. Yuan, M. B. Salamon, R. Movshovich, J. L. Sarrao, and J. D. Thompson, Nature **440**, 65 (2006).
[22] H. Q. Yuan, F. M. Grosche, M. Deppe, C. Geibel, G. Sparn, and F. Steglich, Science **302**, 2104 (2003).
[23] H. Luetkens, H. H. Klauss, M. Kraken, F. J. Litterst, T. Dellmann, R. Klingeler, C. Hess, R. Khasanov, A. Amato, C. Baines, M. Kosmala, O. J. Schumann, M. Braden, J. Hamann-Borrero, N. Leps, A. Kondrat, G. Behr, J. Werner, and B. Büchner, Nature Mater. **8**, 305 (2009).
[24] H. Chen, Y. Ren, Y. Qiu, W. Bao, R. H. Liu, G. Wu, T. Wu, Y. L. Xie, X. F. Wang, Q. Huang, and X. H. Chen, Europhys. Lett. **85**, 17006 (2009).
[25] M. Rotter, M. Pangerl, M. Tegel, and D. Johrendt, Angew. Chem. Int. Ed. **47**, 7949 (2008).
[26] S. Nandi, M. G. Kim, A. Kreyssig, R. M. Fernandes, D. K. Pratt, A. Thaler, N. Ni, S. L. Bud'ko, P. C. Canfield, J. Schmalian, R. J. McQueeney, and A. I. Goldman, Phys. Rev. Lett. **104**, 057006 (2010).
[27] S. Sharma, A. Bharathi, S. Chandra, V. R. Reddy, S. Paulraj, A. T. Satya, V. S. Sastry, A. Gupta, and C. S. Sundar, Phys. Rev. B **81**, 174512 (2010).
[28] S. Jiang, H. Xing, G. F. Xuan, C. Wang, Z. Ren, C. M. Feng, J. H. Dai, Z. A. Xu, and G. H. Cao, J. Phys.: Condens. Matter. **21**, 382203 (2009).
[29] R. Khasanov, M. Bendele, A. Amato, P. Babkevich, A. T. Boothroyd, A. Cervellino, K. Conder, S. N. Gvasaliya, H. Keller, H. H. Klauss, H. Luetkens, V. Pomjakushin, E. Pomjakushina, and B. Roessli, Phys. Rev. B **80**, 140511 (2009).
[30] T. J. Liu, J. Hu, B. Qian, D. Fobes, Z. Q. Mao, W. Bao, M. Reehuis, S. A. J. Kimber, K. Prokeš, S. Matas, D. N. Argyriou, A. Hiess, A. Rotaru, H. Pham, L. Spinu, Y. Qiu, V. Thampy, A. T. Savici, J. A. Rodriguez, and C. Broholm, Nature Mater. **9**, 718 (2010).
[31] N. Katayama, S. Ji, D. Louca, S. H. Lee, M. Fujita, T. J. Sato, J. S. Wen, Z. J. Xu, G. D. Gu, G. Y. Xu, Z. W. Lin, M. Enoki, S. Chang, K. Yamada, and J. M. Tranquada, J. Phys. Soc. Jpn. **79**, 113702 (2010).
[32] C. de La Cruz, Q. Huang, J. W. Lynn, J. Li, W. Ratcliff II, J. L. Zarestky, H. A. Mook, G. F. Chen, J. L. Luo, N. L. Wang, and P. Dai, Nature **453**, 899 (2008).
[33] Q. Huang, Y. Qiu, W. Bao, M. A. Green, J. W. Lynn, Y. C. Gasparovic, T. Wu, G. Wu, and X. H. Chen, Phys. Rev. Lett. **101**, 257003 (2008).
[34] W. Bao, Y. Qiu, Q. Huang, M. A. Green, P. Zajdel, M. R. Fitzsimmons, M. Zhernenkov, S. Chang, M. H. Fang, B. Qian, E. K. Vehstedt, J. H. Yang, H. M. Pham, L. Spinu, and Z. Q. Mao, Phys. Rev. Lett. **102**, 247001 (2009).

[35] S. Li, C. de La Cruz, Q. Huang, Y. Chen, J. W. Lynn, J. Hu, Y. L. Huang, F. C. Hsu, K. W. Yeh, M. K. Wu, and P. C. Dai, Phys. Rev. B **79**, 54503 (2009).
[36] A. D. Christianson, E. A. Goremychkin, R. Osborn, S. Rosenkranz, M. D. Lumsden, C. D. Malliakas, I. S. Todorov, H. Claus, D. Y. Chung, M. G. Kanatzidis, R. I. Bewley, and T. Guidi, Nature **456**, 930 (2008).
[37] M. D. Lumsden, A. D. Christianson, D. Parshall, M. B. Stone, S. E. Nagler, G. J. MacDougall, H. A. Mook, K. Lokshin, T. Egami, D. L. Abernathy, E. A. Goremychkin, R. Osborn, M. A. McGuire, A. S. Sefat, R. Jin, B. C. Sales, and D. Mandrus, Phys. Rev. Lett. **102**, 107005 (2009).
[38] S. Chi, A. Schneidewind, J. Zhao, L. W. Harriger, L. Li, Y. Luo, G. Cao, Z. Xu, M. Loewenhaupt, J. Hu, and P. Dai, Phys. Rev. Lett **102**, 107006 (2009).
[39] S. Li, Y. Chen, S. Chang, J. W. Lynn, L. Li, Y. Luo, G. Cao, Z. Xu, and P. Dai, Phys. Rev. B **79**, 174527 (2009).
[40] Y. Qiu, W. Bao, Y. Zhao, C. Broholm, V. Stanev, Z. Tesanovic, Y. C. Gasparovic, S. Chang, J. Hu, B. Qian, M. H. Fang, and Z. Q. Mao, Phys. Rev. Lett. **103**, 67008 (2009).
[41] L. Zhang, D. J. Singh, and M. H. Du, Phys. Rev.w B **79**, 12506 (2009).
[42] A. J. Drew, C. Niedermayer, P. J. Baker, F. L. Pratt, S. J. Blundell, T. Lancaster, R. H. Liu, G. Wu, X. H. Chen, I. Watanabe, V. K. Malik, A. Dubroka, M. Rössle, K. W. Kim, C. Baines, and C. Bernhard, Nature Mater. **8**, 310 (2009).
[43] B. Sales, A. Sefat, M. McGuire, R. Jin, D. Mandrus, and Y. Mozharivskyj, Physical Review B **79**, 094521 (2009).
[44] A. Martinelli, A. Palenzona, M. Tropeano, C. Ferdeghini, M. Putti, M. R. Cimberle, T. D. Nguyen, M. Affronte, and C. Ritter, Phys. Rev. B **81**, 094115 (2010).
[45] T. Taen, Y. Tsuchiya, Y. Nakajima, and T. Tamegai, Physical Review B **80**, 092502 (2009).